ASPS Conference Proceedings 1: 673-685 (2022)

Proceedings of

12th Structural Engineering Convention-An International Event (SEC 2022)

Available at https://asps-journals.com/index.php/acp

Application of MR damper in Base-isolated Irregular Building with different variable sliding Isolators

Ajay Sharma [1, *], Sudhir Kumar Soni [2]

[1] Professor, Dept. of Structural Engineering, MBM Engineering College, Jodhpur, Corresponding author (Email: ajayvidyanand@gmail.com)
[2] Ph.D. Scholar; Dept. of Structural Engineering, MBM Engineering College, Jodhpur

Paper ID - 060182

Abstract

Application of Electromagnetic induction (EMI) based passively controlled and some local response governed MR dampers in controlling the isolator displacement in base-isolated Irregular building have been studied and compared with the Lyapunov controller. The Irregular building is hybrid isolated with elastomeric rubber bearings and a variety of sliding isolators subjected to strong near field earthquakes acting bi-directionally in horizontal plane. The shear type base-isolated Irregular building is modelled as three-dimensional linear elastic structure having three degrees-of-freedom at each floor level. Time domain dynamic analysis of the building has been carried out using constant-average acceleration Newmark-Beta method and non-linear isolation forces has been taken care by fourth-order Runge-Kutta method. It is observed that the EMI based passive controller performs better than the Lyapunov controller though it reduces less base displacement but gives lower structural response among all the controllers. Local response governed Hyperbolic and Aly's controller require only velocity and displacement at controller locations sound simpler in application as compared to Lyapunov controller especially to civil engineering structures like Irregular building. The Hyperbolic controller restrains base displacement comparable to the Lyapunov controller but gives less base shear and story drifts to Irregular building. Variable frequency pendulum isolator (VFPI) and variable curvature friction pendulum system (VCFPS) sliding isolators perform better with MR damper control in comparison to conventional friction pendulum system (FPS) in base–isolated Irregular building.

Keywords: Base isolation; Semiactive control; Smart passive control; MR dampers; Sliding isolators; Irregular building

1. Introduction

A large number of approaches and technologies to attenuate seismic response of buildings have been developed over the years. The motif of seismic control techniques is to improve performance of structural and non-structural components of such buildings. Base isolation has been proved as an efficient technique to protect the structures against earthquakes. The flexible layer of base isolation decouples the superstructure from the shaking ground so that it behaves almost like a rigid body with low inter-story drifts and floor accelerations. Besides the benefits in the improvement of seismic response of superstructure, large base displacement at isolation level is the worry of such structures especially when they are subjected to near field earthquakes [1-3]. During the last two decades, an ever-increasing database of recorded ground motions have demonstrated that the kinematics characteristics of the ground motion near the faults of major earthquakes contain large displacement pulses, say one or two pulses from 0.5 m to more than 1.5 m with peak velocity of 0.5 m/sec or higher. Their period is usually in the range of 1 to 3 sec, but it can be as long as 6 sec. Such distinct pulses do not exist in ground motions recorded at locations away from the near-fault region, i.e., El Centro, 1940 earthquake ground motion. These near-field earthquakes proved highly catastrophic so base isolation technique independently may prove insufficient thus application to additional control devices is absolutely necessary.

These additional control devices reduce large base displacement, but in addition there is fall in super structural performance especially in inter-storey drifts and floor accelerations. The additional control devices can be based on passive, active and semiactive control. Passive control devices like passive viscous or friction dampers though do not require external power but due to their constant characteristic response to highly varying earthquake loading limit their performance, thus they may fail to achieve desired level of control. Active control devices require huge source of power supply for their electro-hydraulic or electromechanical actuator which may not available constantly in the event of catastrophe. On one hand the occurrence of earthquakes in the designed life of structures may not be quite frequent and on other hand the stability and robustness of active controllers are yet to be established thus employment and maintenance of such control devices can be unfeasible. In such situations application of semiactive control devices is suitable solution as they are not only

*Corresponding author. Tel: + 919414106027; E-mail address: ajayvidyanand@gmail.com

© 2022 The authors. Published by Alwaha Scientific Publishing Services, ASPS. This is an open access article under the CC BY license.

Published online: December19, 2022
doi:10.38208/acp.v1.568

robust and reliable as passive controllers but devoid of ills of active controllers also.

Semiactive control devices are basically passive devices in which their constant characteristic properties can be effectively controlled by some control mechanisms and small amount of power. These devices are not only adequately efficient as active control devices but also highly reliable and robust. Several semiactive systems based on variable stiffness, damping and friction devices have been investigated and demonstrated to be effective by many researchers. Some variable damping and variable friction devices have been implemented on base isolated buildings for reducing base displacements and superstructure responses [4-11].

Use of Magnetorheological (MR) fluid dampers in semiactive control systems is quite popular recently and several researchers have shown that it has been found effective in reducing the response of base isolated structures [12-16]. MR dampers have simple mechanical system, high dynamic range, low power requirement, large force capacity and robustness. MR dampers utilize MR fluid to produce controllable damping force in which the magnitude of damping force is a nonlinear function of voltage and velocity across the damper. The control over the damper force is achieved by changing the voltage input to the damper. Several nonlinear hysteretic models [17-19] have been proposed to describe the force–velocity relationship of the MR damper. These analytical models which describe the behaviour of the damper are very complicated in modelling and controller design. It has also been observed that the nonlinear dampers may result in increased floor accelerations and shears in base isolated buildings in certain earthquakes. MR Dampers have been used in conjunction with a host of model based control algorithms e.g. Lyapunov control [20-21], Bang-bang control [22], Clipped Optimal control [23-24] , Modulated homogeneous friction control [6] and some non-model based intelligent control like Fuzzy and Neuro-fuzzy control laws [25-26] . A majority of the control algorithms developed result in on–off switching laws. Though these algorithms are effective in reducing base displacements, in many cases the benefits are achieved at the cost of increase in floor accelerations and inter-storey drifts. The increase in the super-storey accelerations and inter-storey drifts are a result of the abrupt switching; smooth switching algorithms alleviate the problem to a large extent. Also, all these control algorithms require feedback control system consisting of a controller, sensors, and a power supply. Thus, this semiactive system is usually not only relatively expensive as compared to passive system but also not easy to implement and maintain for large-scale structures such as high-rise buildings and long-span bridges.

To resolve the difficulties of handling such immense sensor data, the need is to have such control strategies which depend either on local responses or can passively control MR damper. In this paper a study has been carried out to evaluate the effectiveness of such simple and passive controller laws which either control the MR damper passively or regulate control through displacement and velocity of the damper. One such smart passive control system that consists of an MR damper and an electromagnetic induction (EMI) part was proposed by Cho et al. [27]. In the smart passive system, the damping characteristics of a damper can be changed by the EMI part consisting of a permanent magnet and a coil according to Faraday's law of EMI. Another Hyperbolic control law [28] in which control over damping is exercised through a Hyperbolic passive function controlling input voltage using velocity of the damper. The simplicity of the Hyperbolic law is it requires single local response and gives efficient control over damping. Aly's algorithm [29] is also one such control law which requires the two local responses i.e. displacement and velocity at damper location and it has been observed that this controller effectively control inter-story drifts and absolute floor accelerations.

The present study investigate the effectiveness of simple control laws based on local responses and passively controlled MR damper in comparison to Lyapunov control for seismic response of base-isolated Irregular building which is isolated primarily with sliding isolators like Friction pendulum system (FPS), Variable frequency pendulum isolator (VFPI) and Variable curvature friction pendulum system (VCFPS). The specific aims of the study are (i) to study the comparative performances of EMI, Hyperbolic law and Aly's controller with Lyapunov controller for seismic control of base-isolated bench mark building and (ii) to compare the performances of FPS, VFPI and VCFPS sliding isolators with MR damper based semiactive control in base-isolated Irregular building.

2. Smart base-isolated irregular building isolated with sliding isolators

The asymmetric base-isolated Irregular building is eight-storied steel-braced framed, 82.4m long and 54.3m wide [30]. The bearing level plan of the L-shaped asymmetric building is shown in Figure 1(a). The isolation system

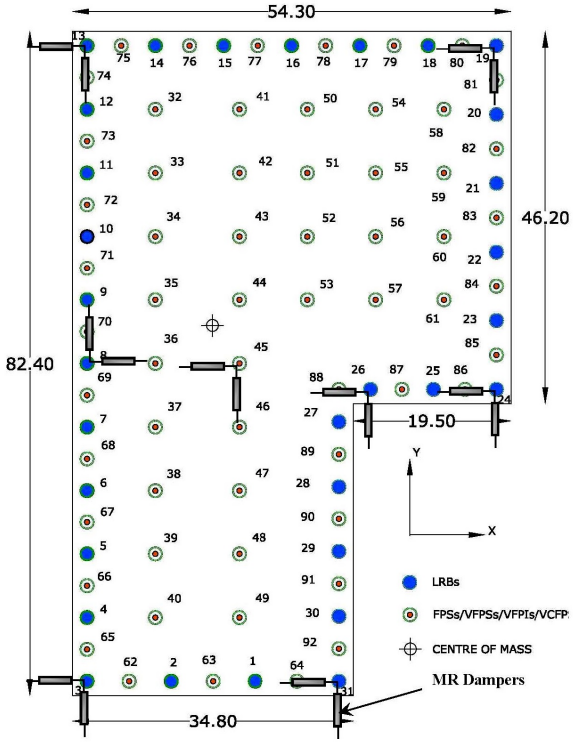

Fig.1(a) Bearing Level Plan of Irregular Building

consists total 92 isolators out of which 61 are sliding isolators which can be FPS or VFPI or VCFPS and 31are linear elastomeric rubber bearings (ERB). In additional 16 MR dampers (8 in x direction and 8 in y direction) located at isolation level to check base displacement as shown in the Figure 1 (a).

The isolators are connected between these drop panels and the footings below. The superstructure is modelled as a three-dimensional linear elastic shear structure. Floor slabs and the base mat are assumed to be rigid in plane. The superstructure and the base are modelled using three multi degrees of freedom (DOF) per floor at the center of mass. The combined model of the superstructure (24 DOF) and isolation system (3 DOF) consists of total 27 DOF. The superstructure damping ratio is assumed to be 5 percent in all fixed-base modes.

The three-dimensional dynamic analysis of the base-isolated Irregular building is carried out considering superstructure condensed linear-elastic, as for base-isolated buildings superstructures can be considered remain elastic. The non-linear isolation bearing is modelled explicitly using the discrete biaxial Bouc–Wen model and the forces in the bearings are transformed to the center of mass of the base using a rigid base slab assumption. All the isolation bearings are modelled individually or globally by equivalent lumped elements at the center of mass of the base. The fundamental period of isolation system consisting ERBs and sliding isolators is 3 sec. The characteristic damping ratio (ζ) of ERB is kept 0.05. The coefficient of friction (μ) for all the sliding isolator has been taken as 0.06.

Varying curvature sliding isolators have variable radius of curvature of sliding surface in comparison to fixed radius of curvature of FPS, which reduces on increasing isolator displacement so as to soften the restoring force component and eventually the isolator force. The reduction in isolator force leads to improve the floor accelerations, inter-story drifts, and related structural response. VFPI [31-32] and VCFPS [33-34] are the two varying curvature sliding isolators developed in the recent past. It has been found that the VFPI and VCFPS performed comparatively better in the near fault area as far as the structural response is concerned except, they give large isolator displacement. The characteristic of VFPI has been chosen as the initial time period (Ti) and frequency variation factor (fvf) are equal to 2 sec and 1 respectively. Similarly, the initial time period (Ti) and the distance from centre the slider can be brought back (r0) are equal to 2 sec and 0.8 m respectively for VCFPS. The details regarding the dynamic equation of base-isolated Irregular building and VFPI and VCFPS can be obtained from the above cited references.

3. Mechanical model of the MR Damper

Electrorheological (ER) and Magnetorheological (MR) fluids are controllable fluids which have ability to reversibly change from a free-flowing, linear viscous fluid to a semi-solid with controllable yield strength in milliseconds when exposed to an electric or magnetic field. The developments of theses fluids gave birth to ER and MR Dampers which proved effective devices work on the principles of semiactive control. The configuration of a 20-ton MR damper developed by Lord® is shown schematically in Figure 2.

As the damper piston moves, the MR fluid is forced through an annular orifice can offer an attractive compromise between the (the 'MR valve'), which is exposed to a magnetic field generated by a coil. MR fluids are the magnetic analogs of electrorheological fluids and typically consist of micron-sized, magnetically polarizable particles dispersed in a carrier medium such as mineral or silicone oil. When a magnetic field is applied to the fluids, particle chains form, and the fluid becomes a semi-solid and exhibits visco-plastic behaviour similar to that of ER fluids. The formation of particle chains that increase the resistance to fluid enables the development of a controllable damping force as shown in Figure 3 (a).

A typical force-displacement and force–velocity relationship for an MR damper under different magnetic fields are shown in Figure 3 (b) and 3 (c). Various applications of MR dampers damper have been considered, such as the seismic control of bridges and tall buildings etc.

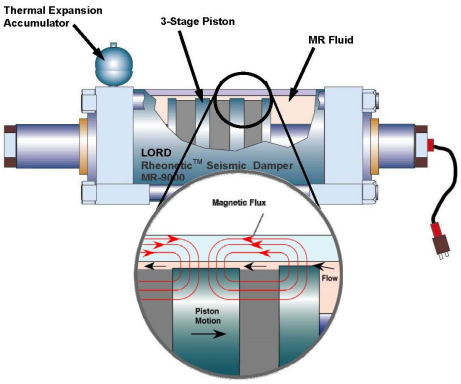

Fig.2 20 Ton MR Damper

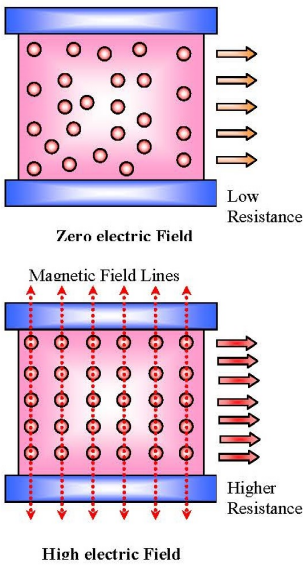

Fig.3(a) Formation of Plastic Chain

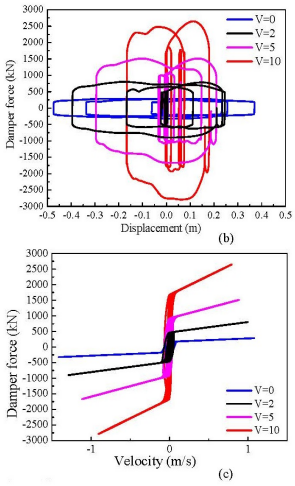

Fig. 3(b) and 3(c) Force-Displacement and Force-Velocity Relationship

The MR dampers show dynamically non-linear force-velocity behaviour, hence more accurate dynamic model of MR dampers is necessary. Also modelling of the control devices is essential for the adequate prediction of the behaviour of the controlled system. Several models have been proposed to describe the behaviour of MR dampers. These include the phenomenological model based on the Bouc-Wen hysteresis model proposed by Spencer et al., [35], neural network model developed by Chang and Roschke [36], viscoelastic-plastic model [37], fuzzy model [38], polynomial model [39]. Among these MR models, Modified Bouc-Wen model proposed by Spencer et al. [35] can accurately describe the behaviour of the MR dampers thus for the present study it has been used which is described in the following relationship between force and velocity

$$f = c_1\dot{y} + k_1(x_d - x_0) \tag{1}$$

$$\dot{z} = \gamma|\dot{x}_d - \dot{y}|z|z|^{n-1} - \beta(\dot{x}_d - \dot{y})|z|^n + A(\dot{x}_d - \dot{y}) \tag{2}$$

$$\dot{y} = \frac{1}{(c_0 + c_1)}\{\alpha z + c_0\dot{x}_d + k_0(x_d - y)\} \tag{3}$$

where z is an evolutionary variable that accounts for the history dependence of the response; x_d is the damper displacement; $\dot{x}_d$ is the velocity across the damper; k1 is the accumulator stiffness; c1 is viscous damping at lower velocity in the model to produce the roll-off; c0 is viscous damping at larger velocity; k0 is the stiffness at large velocity; and x_0 is the initial displacement of spring; and α, β, γ, n and A are the shape or characteristic parameters of the model. The model parameters α , c0 and c1 depend on the voltage to the current driver as follows

$$\alpha = \alpha_a + \alpha_b u \tag{4}$$

$$c_1 = c_{1a} + c_{1b}u \tag{5}$$

$$c_0 = c_{0a} + c_{0b}u \tag{6}$$

while the filtered voltage u determined by the applied voltage v to the control circuit is as follows

$$\dot{u} = \eta(u - v) \tag{7}$$

where η is a constant in Equation (7) is necessary to model the dynamics involved in reaching rheological equilibrium and in driving the electromagnet in the MR damper. The optimized parameters for the dynamic model those were determined to best fit the data based on the experimental results of a 20-ton MR fluid damper [40] and used in the present study. The optimized parameters for the dynamic model those were determined to best fit the data based on the experimental results of a 20 ton MR fluid damper and used in the present study are as follows: α_a =46.2 kN/m; α_b =41.2 kN/m/v; c_{0a} =110 kN-s/m; c_{0b} =114.3 kN-s/m/v; c_{1a} =8359.2 kN-s/m; c_{1b} =7482.9 kN-s/m/v; k_0 =0.002 kN/m; k_1 =0.0097 kN/m; γ=164 m-2; β=164 m-2; A =1107.2 and n=2.

4. Semiactive control strategies for MR Dampers

A variety of approaches have been used in the proposed study for the control of MR dampers. In developing these control laws, the control voltage is restricted in the range of 0-10 volts.

4.1 Lyapunov Stability Theory Based Control Algorithm

This approach requires the use of a Lyapunov function. Even though numbers of Lyapunov functions are available, but here Lyapunov's direct approach is used. In which a positive definite matrix P is found with selected positive semi-definite matrix Q_P and system matrix A by using the following Lyapunov equation [41].

$$A^T P + PA = -Q_P \tag{8}$$

The control law that determines the current sent to i^{th} MR damper as follows

$$v_i = V_{\max} H((-z^T)PB_i f_{di}) \tag{9}$$

where V_{max} is the maximum voltage; H (.) is the Heaviside step function; f_{di} is measured force at the i^{th} MR damper and B_i is the i^{th} column of system matrix B of the structure. This algorithm, better perform when measurements of the responses of the full structure are used which means that it requires large number of sensors.

4.2 Electromagnetic Induction (EMI) Based Passive Control of MR Damper

Generally, MR damper-based control systems are governed by the feedback control which requires number of sensors, controllers and power supply units and when number of MR dampers increases, the control system become quite complex and costly as well. To avoid such problems Cho *et al.,* [27] proposed EMI based smart passive control system can be a better answer. The smart passive system contains an MR damper and an EMI system. The EMI system

comprises a permanent magnet and solenoid coils attached to MR damper as shown in Figure 4 (b). According to the Faraday law of induction [42-44], the EMI system changes the kinetic energy of the reciprocation motion of the MR damper to electric energy for the MR damper and then the electric energy is used to change the damping characteristics of an MR damper by forming magnetic field in the damper. Thus, the MR damper with EMI system is a passive system that does not require any power at all. Furthermore, the induced electric energy is proportional to external loads like earthquakes, which means that the smart passive system is adaptable to external loads by itself without any controller or corresponding sensors. General passive systems lack this adaptability whereas the MR damper with EMI system is an intelligent passive system to overcome shortcomings of general passive systems. These are important benefits of using the smart passive system.

The electromotive force (i.e. EMF) produced by motion of a structure can be expressed by the Faraday's law of induction as

$$\varepsilon = -kN\frac{d\Phi_B}{dt} = -kNBw\frac{dx}{dt} = -k_{emf}\frac{dx}{dt} \qquad (10)$$

where ε is the induced EMF that has unit of volt (v), k is the energy loss coefficient factor, B is the magnetic flux density that has unit of Tesla (T=Wb/m^2), N is the number of turns of the coil, w is the width of the magnet, and x is the displacement of the coil. Here, the energy loss coefficient factor, k, is caused by the difference between the theoretical values obtained by Faraday's law and the real experiments due to differences of coil length corresponding to the number of turns, the magnitude of the permanent magnet between N and S poles, and k_{emf} is known as appropriate gain of the EMI and so on. As per Equation (10) faster movement of MR damper produce higher EMF and vice-versa. This induced EMF is carried to an electromagnet in the piston head and generates magnetic field around the electromagnet that changes the damping characteristics of the MR fluid (refer Figure 4 (b)).

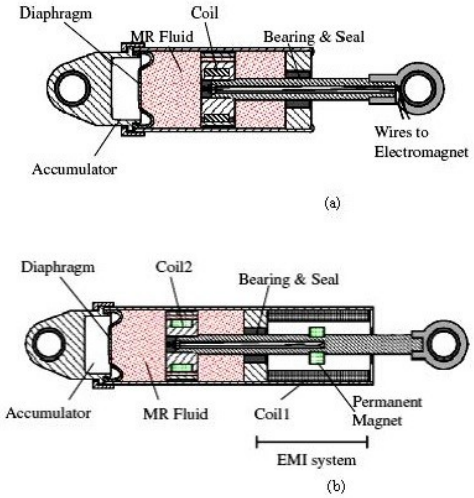

Fig. 4(a) &4(b) MR Damper

In real cases, because the external loads such as earthquakes and winds cause the reciprocal motion of the MR damper, the solenoid coil of the EMI device moves back and forth for inducing EMF, which generates the adaptable power and adjusts to the vibration of structures by itself without any controller or corresponding sensors.

4.3 Hyperbolic Control Algorithm

Pozo *et al*., [28] proposed a voltage control law for the MR damper which requires only local velocity where the damper is connected. The controller which give smooth command voltage is a Hyperbolic function of the local velocity $(\dot{x})$ and expressed as

$$u_c = \frac{\sec h(\dot{x})\tan h(\dot{x})\,\mathrm{sgn}(\dot{x})}{1+|\dot{x}|} \qquad (11)$$

The above controller can very easily produce the force velocity relationship of the MR damper. The simplicity of the above expression suggests the possibility of a purely passive implementation can be possible if the appropriate control to feed the command voltage is made available.

4.4 Aly's Control Algorithm

A new voltage control law which also requires only local responses is proposed by Aly [29]. The local responses are the relative displacement (x) and velocity $(\dot{x})$ of the location where the MR damper is connected and which is expressed as

$$v_i = \begin{cases} \alpha V_{\max} & if \quad sign(x)=1 \quad and \quad sign(\dot{x})=1 \\ \beta V_{\max} & if \quad sign(x)=-1 \quad and \quad sign(\dot{x})=-1 \\ \gamma V_{\max} & if \quad sign(x)=1 \quad and \quad sign(\dot{x})=-1 \\ V_{\max} & Othervise \end{cases} \qquad (12)$$

where the values of the constants α, β, and γ should be chosen between 0 and 1 so as to have better hysteresis loop of the MR damper.

5. NUMERICAL STUDY

The time domain dynamic analysis has been conducted on the computational model of base-isolated Irregular building to investigate the comparative performances of the different control laws based on local responses and passive controlled MR damper with Lyapunov controller. Also, various isolation systems comprising FPS or VFPI and VCFPS isolators with MR dampers in controlling the seismic response of the base-isolated Irregular building have also been compared. The Irregular building is acted upon by seven strong earthquake ground motions acting bi-directionally in the horizontal directions ignoring vertical component of ground motions. The historical earthquakes which are used in the study, are the 1994 Northridge *Newhall* Station (360 as Fault-Normal and 90 as Fault-Parallel); 1994 Northridge *Sylmar* Station (360 as Fault-Normal and 90 as Fault-Parallel); 1940 Imperial Valley-*El Centro* Array # 9 (180 as Fault-Normal component and 270

as Fault-Parallel component); 1994 Northridge *Rinaldi* Station (228 as Fault-Normal and 318 as Fault-Parallel); 1995 *Kobe*-JMA Station (KJM 000 component as Fault-Normal and KJM 90 component as Fault-Parallel), 1999 Taiwan *Jiji* TCU 068 station (N as Fault-Normal and W as Fault-Parallel) and 1995 *Erzincan* (Turkey) (NS as Fault-Normal and EW as Fault-Parallel). The Modified earthquake time histories of above earthquakes with time step 0.001 sec for 30 sec are used for the present study. All the earthquake ground motions are applied bi-directionally to the building, in which the fault normal component is applied in *x*-direction and fault parallel component is applied in *y*-direction.

The present study is focused on time history responses and peak performance criteria of absolute floor acceleration, base displacement, base shear and story drift of base isolated Irregular building for comparing the performances of control laws and isolation systems. The peak performance criteria, are J_1 = Peak base shear of base-isolated Irregular building/corresponding value of non-isolated Irregular building; J_2 = Peak story shear of base-isolated Irregular building/corresponding value of non-isolated Irregular building; J_3 = Peak base displacement of base-isolated Irregular building; J_4= Peak story drift of base-isolated Irregular building/corresponding value of non-isolated Irregular building; J_5 = Peak absolute acceleration of base-isolated Irregular building/corresponding value of non-isolated Irregular building; J_6 = Peak Control force at the centre of base mat of base-isolated Irregular building/total weight of the Irregular building; J_7 = Root mean square (RMS) base displacement of base-isolated Irregular building ; J_8 = Root mean square (RMS) absolute acceleration of base-isolated Irregular building/corresponding value of non-isolated Irregular building; J_9 =Total energy absorbed by the semiactive dampers/ input energy and J_{10} =Maximum cumulative control force/ maximum cumulative isolator force. For evaluating the above performance evaluation criteria, the structural response quantities are normalized by their corresponding non-isolated/ fixed base values in comparison to isolated values as in case of the base-isolated Irregular building, because the present study aims to evaluate the relative performance of different isolation systems primarily besides the comparative effectiveness of different control laws of MR dampers.

The numerical study carried out on hybridly base-isolated building which has 31 ERB and remaining 61 are either FPS or VFPI or VCFPS in the isolation systems. MR dampers are positioned at eight different locations both in *x* and *y* directions as shown in Figure 1 to check the large base displacement. The MR dampers are controlled by Lyapunov controller, smart passive control using EMI, Hyperbolic control and Aly's controller. Besides applications of MR damper with above controllers, the passive off and the passive on cases in which constant command voltage 0 and 10 volts have been observed for the purpose of comparison. The constants of different control laws are chosen so as to have adequate reduction in base displacement without inordinate increase in floor accelerations and story drifts. The k_{emf} for EMI based control has been take equal to 5 and α, β, and γ for Aly's control have been chosen as 1, 0.5 and 0.5 respectively. Although it is suggested that selection of constants should be chosen optimally for a particular system so as to have effective performance of the controller.

The absolute floor acceleration is the important structural response parameter to manifest the efficiency of seismic control system applied to any building. Figure 5 shows the time history responses of top floor absolute accelerations in x direction of FPS isolated (31ERB+61 FPS) Irregular building subjected to the Northridge Sylmar earthquake for different controllers. A small table associated with the Figure 5 gives the peak values of top floor absolute accelerations for the different controllers and for the uncontrolled (without MR dampers) case as well.

It shows that in comparison to Lyapunov controller, EMI based passive control gives lower acceleration response among the entire controllers. Hyperbolic controller performs at par with Lyapunov controller whereas the Aly's controller gives much higher acceleration response among the entire controllers. Figure 6 and 7 show the similar top floor absolute acceleration with VFPI and VCFPS isolated Irregular building and it has been observed that these isolation systems give little higher floor acceleration than FPS isolation for all the controllers.

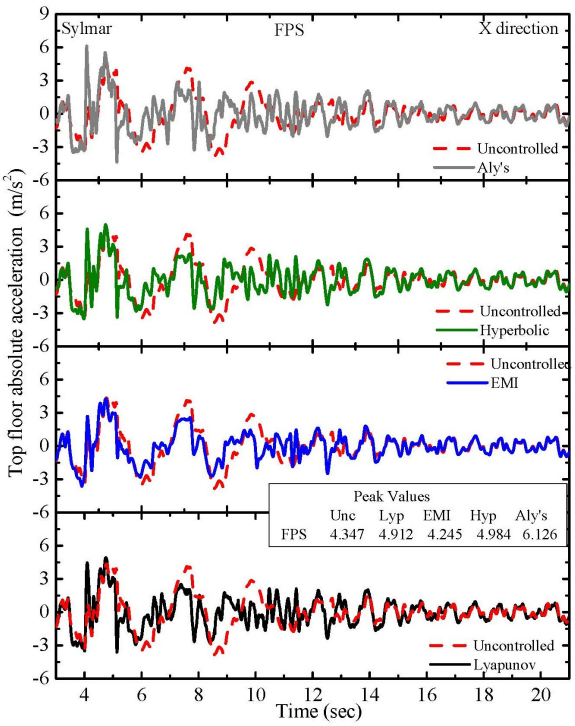

Fig.5 Peak values of top floor absolute accelerations for the different controllers and for the uncontrolled (without MR dampers)

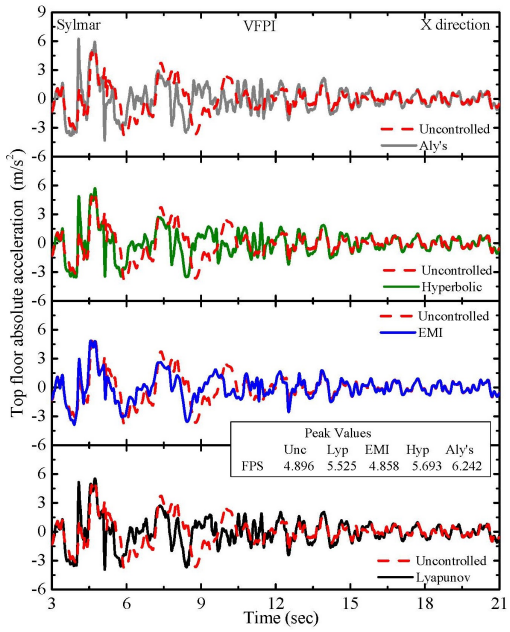

Fig.6 Top floor absolute acceleration with VFPI

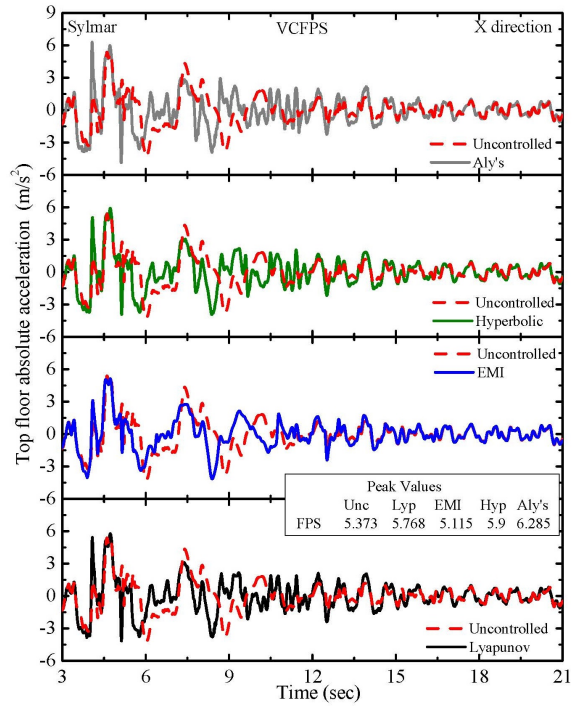

Fig.7 Top floor absolute acceleration with VCFPS

It is because their uncontrolled accelerations are also higher from them and since the more reduction in base displacement gives increase in the floor acceleration. Table 1 which gives the peak normalized absolute floor acceleration for all the seven earthquakes and for controlled and uncontrolled cases.

Table-1 Peak normalized absolute floor acceleration

Table 1

	Control Type	Normalized peak absolute floor acceleration (J_3)						
		Newhall	Sylmar	El Centro	Rinaldi	Kobe	Jiji	Erzincan
FPS	Uncontrolled	0.19719	0.26588	0.48675	0.1856	0.12551	0.48674	0.22926
	Passive Off	0.21945	0.31447	0.54776	0.18818	0.14642	0.44201	0.22793
	Passive On	0.35472	0.5796	0.79949	0.27331	0.28319	0.43266	0.39107
	Lyapunov	0.30505	0.44368	0.67166	0.21272	0.21762	0.40701	0.31113
	EMI	0.23826	0.33469	0.55776	0.18131	0.16463	**0.36638**	**0.20705**
	Hyperbolic	0.2897	0.48406	0.66678	0.19933	0.22204	0.38065	0.2814
	Aly's	**0.31885**	**0.51727**	**0.77623**	**0.23314**	**0.24657**	0.38061	0.34437
VFPI	Uncontrolled	0.16891	0.27454	0.47502	0.15131	0.11415	0.39403	0.23626
	Passive Off	0.18317	0.29561	0.53479	0.15599	0.13983	0.40543	0.24822
	Passive On	0.33252	0.56647	0.80143	0.2767	0.26991	0.43116	0.39215
	Lyapunov	0.26852	0.412	0.66651	0.1957	0.19591	0.38941	0.30947
	EMI	0.2008	0.30764	0.54454	**0.17233**	0.14462	0.38553	0.23386
	Hyperbolic	0.25252	0.45994	0.66346	0.19446	0.20804	**0.41428**	0.27905
	Aly's	0.29546	0.48855	0.77639	0.23073	0.23555	0.4026	0.34501
VCFPS	Uncontrolled	0.16824	0.30131	0.47484	0.17201	0.11528	0.49217	0.26328
	Passive Off	0.18076	0.30233	0.53457	0.16896	0.1296	0.39751	0.26953
	Passive On	0.327	0.55729	0.80142	0.27233	0.26727	0.43808	0.39108
	Lyapunov	0.26288	0.39617	0.6666	0.19759	0.19484	0.38182	0.31308
	EMI	**0.18703**	**0.28687**	**0.54432**	0.18136	**0.14263**	0.37692	0.24766
	Hyperbolic	0.24363	0.44278	0.66341	0.1928	0.20591	0.4124	0.2861
	Aly's	0.29177	0.47429	0.77636	0.23137	0.2327	0.41407	**0.35041**

The grey shaded area gives the values for the uncontrolled case when building is only isolated and no MR dampers or other devices to control the base displacement are employed. The yellow shaded area gives the comparative view of values for the different controllers. The bold red and blue values are maximum and minimum values for the corresponding earthquake respectively among the controllers. It is observed that the most of the maximum values are associated with Aly's controller and the smart passive EMI based control gives minimum values for all the earthquakes. It is noted that Aly's controllers give about 10 to 80 percent higher values of peak floor accelerations than EMI control. It has also been noted that the values of normalized peak absolute floor accelerations are comparatively higher for FPS for all the controlled cases in comparison to VFPI and VCFPS (refer Table 1). It is because of the disadvantage of higher isolation force offered by FPS which worsens the structural response. From the above observations it can be concluded that EMI based passive control and Hyperbolic control are better controller than Lyapunov and Aly's controller and VFPI and VCFPS give better acceleration response with MR Dampers in comparison to FPS.

The application of MR dampers to the base-isolated Irregular building is primary to control large base displacement due to near-field earthquakes. The time history plots of base displacement of Irregular building for different isolation cases and controllers comparing the individual responses with uncontrolled case have been shown in Figures 8, 9 and 10. Figure 8 shows the time history plots of FPS isolated Irregular building with MR dampers for different controllers and it is noted that Lyapunov controller better restricts the base displacement in comparison to others.

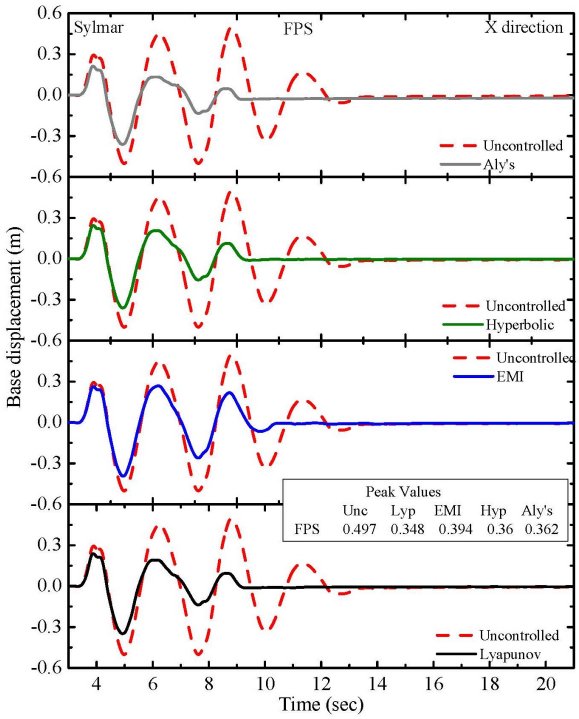

Fig-8 Time history plots of FPS isolated Irregular building

Figure 9 and 10 give base displacement plots for VFPI and VCFPS and it has been observed that Lyapunov controller also perform better for them.

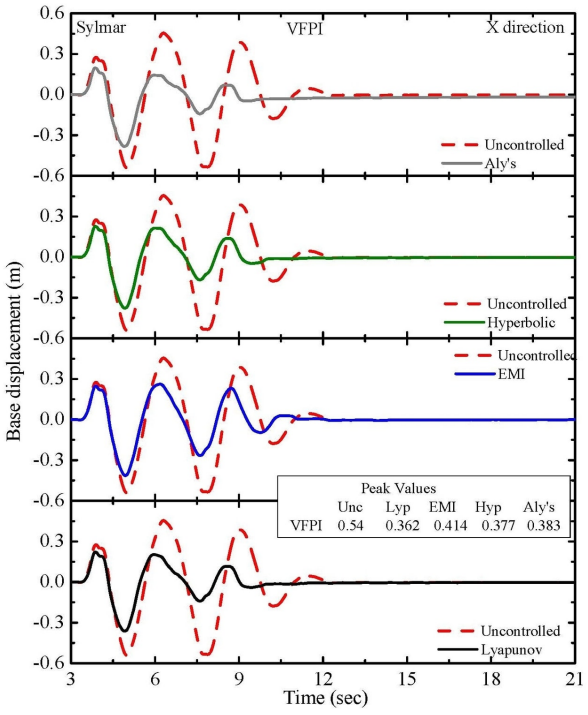

Fig.9 Base displacement plots for VFPI

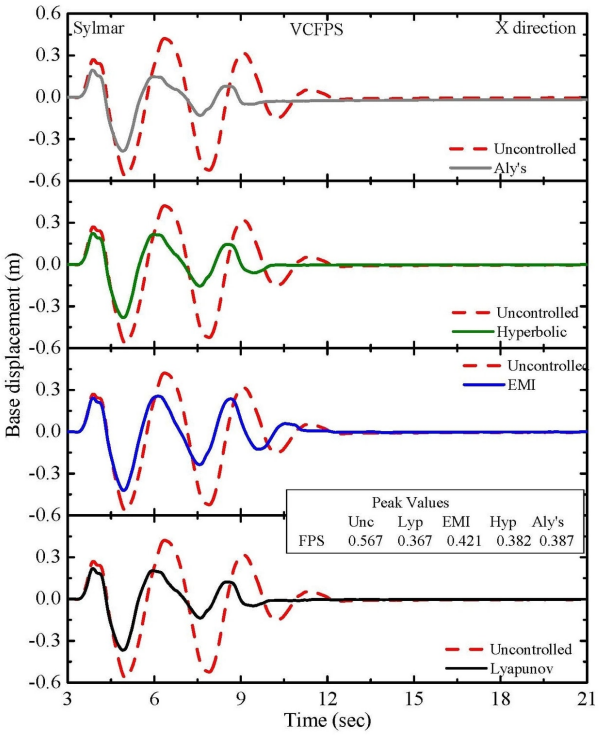

Fig.10 Base displacement plots for VCFPS

It has also learnt that VFPI and VCFPS isolation systems give more base displacement than FPS isolation system with MR dampers. Although the reduction of base displacement due to MR dampers in FPS is around 30 percent where as in VFPI and VCFPS it is in the range of 33 to 36 percent thus MR dampers work better with VFPI and VCFPS. Table 2 which give the peak base displacements of Irregular building for different isolation systems and controllers of MR dampers, show that Aly's controller gives 20 to 35 percent higher reduction around in base displacement among the four controllers in comparison to their respective maximum values. Lyapunov and Hyperbolic also perform better but next to Aly's controller (refer Table 2).

Table- 2 Peak base displacements of Irregular building

Table 2

	Control Type	Peak base displacement (J_1)						
		Newhall	Sylmar	El Centro	Rinaldi	Kobe	Jiji	Erzincan
FPS	Uncontrolled	0.23756	0.50179	0.06912	0.37117	0.21626	0.78836	0.50646
	Passive Off	0.2221	0.47685	0.05553	0.36063	0.19548	0.70104	0.47934
	Passive On	0.13397	0.27829	0.03306	0.30151	0.13558	0.36463	0.29522
	Lyapunov	0.16321	**0.34822**	0.04766	0.32728	**0.1443**	0.48577	0.33857
	EMI	0.20551	0.39375	0.0509	0.32591	0.16836	0.53724	0.38003
	Hyperbolic	0.16935	0.36047	**0.03823**	0.32629	0.16027	0.48757	0.34423
	Aly's	0.17216	0.36186	**0.05747**	**0.28725**	0.16595	0.46858	0.34217
VFPI	Uncontrolled	0.2608	0.54039	0.0628	0.39189	0.21044	0.81647	0.52348
	Passive Off	0.24792	0.51034	0.05179	0.38602	0.20669	0.75275	0.49154
	Passive On	0.13384	0.2888	0.03602	0.33186	0.14552	0.35376	0.27865
	Lyapunov	0.17644	0.3624	0.04031	0.35746	0.16174	0.5037	0.33553
	EMI	0.21555	0.41362	0.04842	0.33801	0.18513	0.56756	0.38554
	Hyperbolic	0.18187	0.37749	0.04087	0.35815	0.1689	0.49503	0.34299
	Aly's	0.15134	0.38318	0.05305	0.29456	0.16864	**0.46836**	0.32752
VCFPS	Uncontrolled	0.27559	0.56684	0.06076	0.3879	0.22535	0.8348	0.56286
	Passive Off	0.25993	0.53105	0.05087	0.38588	0.22025	0.79842	0.5224
	Passive On	0.13588	0.28866	0.03596	0.33658	0.14914	0.34097	0.27159
	Lyapunov	0.18049	0.36692	0.04026	**0.36548**	0.16262	0.4956	0.34548
	EMI	**0.22466**	**0.42109**	0.04847	0.33919	**0.19279**	**0.5861**	**0.40078**
	Hyperbolic	0.18662	0.38176	0.04097	0.36427	0.1684	0.49857	0.35516
	Aly's	**0.14522**	0.38681	0.0527	0.29525	0.17355	0.47039	**0.31933**

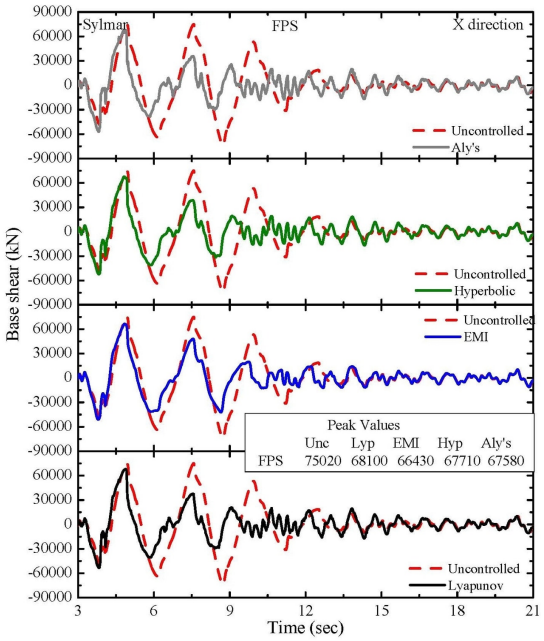

Fig.11 Time history plots for the similar combinations as above for base shear

EMI based passive control gives the least control on peak base displacement among the controllers. Although the reduction is somewhat 10 percent less in EMI controller than Lyapunov but at the same time it gives better performance in floor accelerations and also its unique capability of smart passive control, put it at advantage over Lyapunov controller. Hyperbolic controller exercises almost comparable control over base displacement reduction with Lyapunov controller but lower floor acceleration response than him as observed earlier, prove it better than Lyapunov controller. Aly's controller is observed not as effective as the other controllers as it gives higher floor accelerations though gives better control in base displacement reduction.

The base shear and the story drift are the other two structural response parameters which affect the seismic performance of a building to great extent. Larger base shear and story drift values not only lead damage of the structural and non-structural components but also may cause the complete failure of the entire structure. The time history plots for the similar combinations as above for base shear have shown in Figure 11, 12 and 13.

Figure 11 shows that EMI controller gives least base shear among the entire controllers and Hyperbolic controller also gives less base shear than Lyapunov controller for base-isolated Irregular building for all the isolation systems. From Figures 12 and 13 which show the time history plots for the similar cases for VFPI and VCFPS isolated Irregular building, it is observed that the base shear is 4 to 8 percent less than FPS isolated building for almost all the controllers.

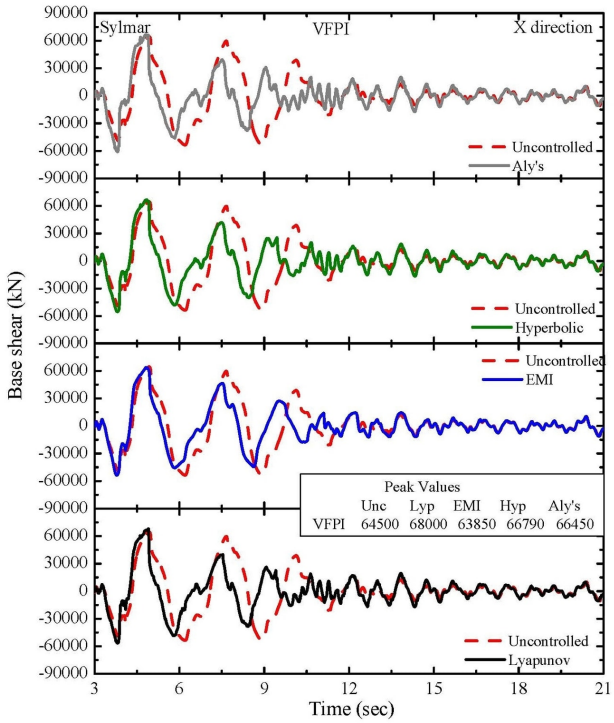

Fig.12 Time history plots for the similar cases for VFPI

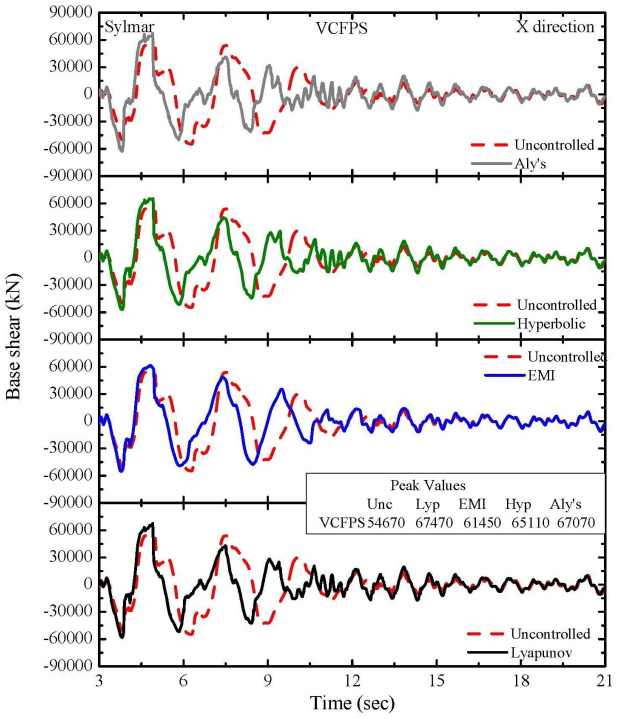

Fig. 13 Time history plots for the similar cases for VCFPS

Table 3 gives the values of normalized peak base shear for different isolation and controlled and uncontrolled cases.

Table-3 Normalized peak base shear

Table 3

	Control Type	Normalized peak base shear (J_1)						
		Newhall	Sylmar	El Centro	Rinaldi	Kobe	Jiji	Erzincan
FPS	Uncontrolled	0.21487	0.37674	0.24966	0.22866	0.13291	0.83901	0.56161
	Passive Off	0.21361	0.37167	0.246	0.22801	0.13166	0.76415	0.55075
	Passive On	0.23443	0.31867	0.41751	0.26396	0.17975	0.58281	0.48595
	Lyapunov	0.20945	**0.34196**	0.33649	0.24785	0.15016	0.59131	0.49258
	EMI	**0.20465**	0.33363	**0.24707**	0.23314	**0.13262**	0.62047	0.47042
	Hyperbolic	0.21012	0.34005	0.31816	0.24866	0.1599	**0.62052**	0.48284
	Aly's	0.2347	0.33941	0.3988	0.24342	0.17932	0.59827	0.48873
VFPI	Uncontrolled	0.22128	0.32391	0.29285	0.21075	0.16087	0.55425	0.46318
	Passive Off	0.22668	0.32821	0.28221	0.21528	0.16905	0.55146	0.47007
	Passive On	0.26233	0.33127	0.45167	0.26919	0.20549	0.55759	0.48678
	Lyapunov	0.24538	0.34165	0.37064	0.24588	0.17448	0.56089	0.48736
	EMI	0.2367	0.32065	0.28919	**0.23138**	0.16875	0.52999	0.46742
	Hyperbolic	0.24056	0.33545	0.36694	0.2492	0.17837	0.53418	0.48223
	Aly's	0.25321	0.33374	0.41122	0.25237	0.1975	0.55171	**0.46658**
VCFPS	Uncontrolled	0.2404	0.27453	0.29568	0.2183	0.17923	0.57991	0.43428
	Passive Off	0.24479	0.2846	0.28423	0.22546	0.18488	0.4681	0.44421
	Passive On	0.27359	0.34123	0.45342	0.27969	0.21549	0.55083	0.50114
	Lyapunov	0.25928	0.33884	0.3733	0.25573	0.18593	0.54462	**0.50004**
	EMI	0.25304	**0.3086**	0.29424	0.23757	0.18294	**0.49457**	0.47599
	Hyperbolic	0.25362	0.32701	0.37088	0.25935	0.18781	0.50766	0.49551
	Aly's	**0.26779**	0.33681	**0.41513**	**0.27106**	**0.20036**	0.5475	0.49867

It is learnt that EMI control performs comparatively better than Lyapunov controller as the increase in peak base shear is 3 to 25 percent lower than Lyapunov controller. Hyperbolic controller also seems to be effective than the Lyapunov controller as values of normalized peak base shear is lower than it but higher than EMI controller. Aly's controller gives most of the maximum values for the peak base shear. The time history plots of story drifts for FPS, VFPI and VCFPS isolated Irregular building for above said cases have been shown in Figure 14, 15 and 16 respectively and on comparing it is noted that EMI controller gives least values among the entire controllers.

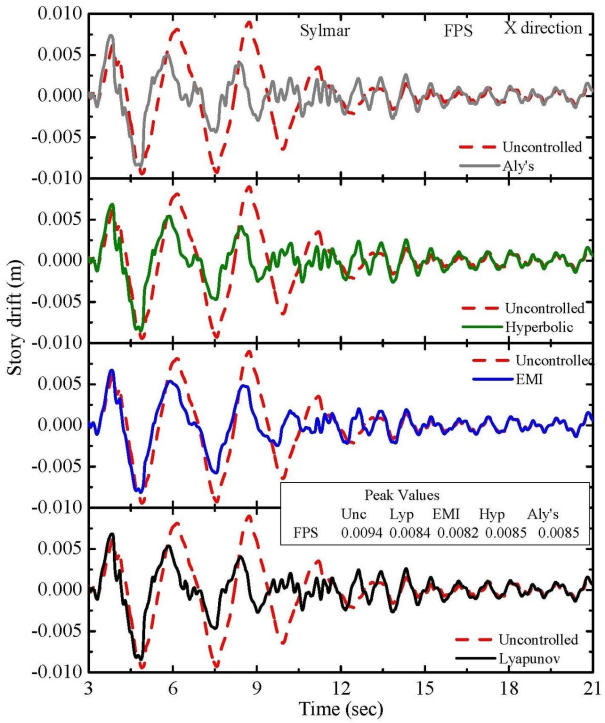

Fig.14 Time history plots of story drifts for FPS

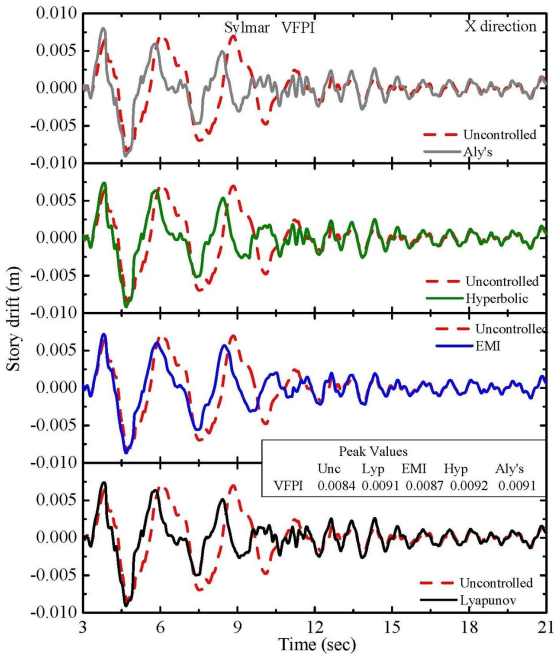

Fig.15 Time history plots of story drifts for VFPI

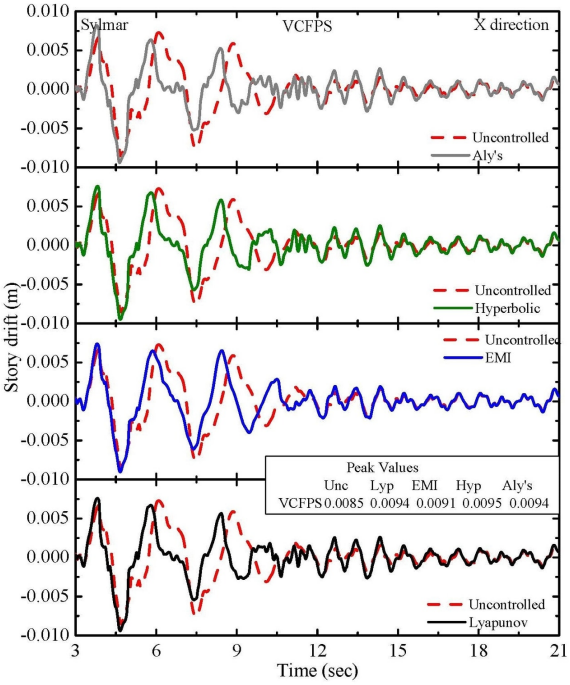

Fig.16 Time history plots of story drifts for VCFPS

Hyperbolic and Lyapunov controller perform almost at par in controlling story drifts. The normalized peak story drifts for all the discussed earlier cases have been given in Table 4 which shows that EMI control restricts 5 to 23 percent more peak story drift in comparison to Lyapunov controller for all the cases.

Table.4 Normalized peak story drifts

Table 4

	Control Type	Normalized peak story drift (J_4)						
		Newhall	Sylmar	El Centro	Rinaldi	Kobe	Jiji	Erzincan
FPS	Uncontrolled	0.22488	0.357	0.34525	0.17039	0.11142	0.66466	0.44273
	Passive Off	0.23269	0.34968	0.38673	0.16887	0.12109	0.55661	0.43059
	Passive On	0.30705	0.37112	0.59893	0.20148	0.21628	0.49201	0.40095
	Lyapunov	0.27558	0.35659	0.52134	0.16822	0.17494	0.43966	0.38664
	EMI	0.24756	**0.33156**	**0.40042**	0.17471	**0.12899**	0.44946	**0.37186**
	Hyperbolic	0.27065	0.36204	0.52963	0.16456	0.16711	0.45767	0.38096
	Aly's	**0.285**	0.3872	0.57798	0.18793	**0.19043**	0.45886	0.37331
VFPI	Uncontrolled	0.20317	0.3989	0.35543	0.14618	0.11165	0.45635	0.40977
	Passive Off	0.20253	0.40634	0.39603	0.14959	0.12025	0.46095	0.41861
	Passive On	0.26716	0.44162	0.6003	0.20875	0.20984	0.51902	0.41757
	Lyapunov	0.22713	0.43077	0.52705	0.16881	0.1831	0.4588	0.42254
	EMI	0.20495	0.40461	0.40908	0.1717	0.1368	0.44413	0.39944
	Hyperbolic	0.22017	0.43749	0.53409	**0.16453**	0.15123	0.45384	0.41696
	Aly's	0.24481	0.44065	0.57964	0.18513	0.17777	**0.4899**	0.40914
VCFPS	Uncontrolled	0.21213	0.43504	0.35575	0.16126	0.12721	0.56601	0.44451
	Passive Off	0.21125	0.44136	0.39628	0.15868	0.12925	0.45202	0.45091
	Passive On	0.26147	0.46408	0.60031	0.21817	0.20812	0.51411	0.44014
	Lyapunov	0.2188	0.45503	0.52723	0.18077	0.18421	**0.43298**	0.45264
	EMI	**0.20014**	0.4323	0.4093	0.17827	0.1377	0.43756	0.43067
	Hyperbolic	0.21102	**0.46437**	0.53416	0.17227	0.15151	0.4477	0.45054
	Aly's	0.23587	0.46279	**0.57966**	**0.19097**	0.17403	0.4876	**0.46158**

From the above observations it can be concluded that EMI and Hyperbolic controller work better than Lyapunov controller and VFPI and VCFPS isolation systems function better with MR dampers in comparison to FPS isolation as far as structural response are concerned.

Controller force and total energy absorbed by the controllers are the two parameters which also play an important part in selecting the semiactive control device and the control algorithm. From Table 5 which shows the controller force for all the above-mentioned cases of controllers and isolation systems, it is observed that EMI control gives 5 to 60 percent less peak control force than the Lyapunov controller.

Table.5 Controller force for all the above-mentioned cases of controllers and isolation systems

Table 5

	Control Type	Normalized peak control force (J_6)						
		Newhall	Sylmar	El Centro	Rinaldi	Kobe	Jiji	Erzincan
FPS	Passive Off	0.01044	0.0128	0.00801	0.01374	0.0105	0.01397	0.01179
	Passive On	0.11147	0.1201	0.08001	0.13769	0.10808	0.10391	0.10622
	Lyapunov	0.07206	0.08141	0.05225	0.09107	0.06818	0.07211	0.07041
	EMI	**0.05379**	0.08796	0.01883	0.10911	**0.05027**	0.06811	0.06006
	Hyperbolic	0.06601	**0.0715**	0.04802	**0.07596**	0.06482	0.06602	0.06499
	Aly's	0.09527	0.10855	**0.08066**	0.13608	0.10077	0.10424	0.10602
VFPI	Passive Off	0.01134	0.01305	0.00785	0.01387	0.01107	0.01303	0.01152
	Passive On	0.11878	0.12276	0.07879	0.13849	0.10958	0.10209	0.1035
	Lyapunov	0.0782	0.08325	0.05156	0.09163	0.07161	0.07056	0.06984
	EMI	0.06823	0.09252	0.01732	0.11127	0.05936	0.06628	**0.05726**
	Hyperbolic	0.06956	0.0723	0.04659	0.07624	0.06564	0.06544	0.06472
	Aly's	**0.09506**	0.10992	0.07992	0.1376	0.10478	**0.10414**	0.10473
VCFPS	Passive Off	0.01175	0.01311	0.00781	0.01394	0.01133	0.01261	0.01163
	Passive On	0.12011	0.12318	0.07871	0.13849	0.10981	0.1012	0.10413
	Lyapunov	0.07952	0.08356	0.05139	0.09194	0.07245	0.07177	0.07113
	EMI	0.07346	0.09341	**0.01698**	0.11248	0.06274	0.06765	0.05759
	Hyperbolic	0.07029	0.07245	0.04645	0.07634	0.06596	**0.06542**	0.06549
	Aly's	0.09495	**0.1105**	0.07976	**0.13784**	**0.10591**	0.10365	**0.10674**

This means that the EMI based control is more efficient than other controllers though it does not require any power to realize these control forces. Hyperbolic controller also operates at lesser control forces than the Lyapunov controller. The total energy absorbed by the MR dampers is given in Table 6.

Table.6 Total energy absorbed by the MR dampers

Table 6

	Control Type	Total Energy absorbed by controllers (J_9)						
		Newhall	Sylmar	El Centro	Rinaldi	Kobe	Jiji	Erzincan
FPS	Passive Off	0.13285	0.15509	0.10954	0.14983	0.13755	0.15812	0.15685
	Passive On	0.53653	0.57401	0.35502	0.60036	0.54492	0.55511	0.60269
	Lyapunov	0.65915	0.75049	0.482	0.66336	0.63314	**0.67803**	0.76501
	EMI	**0.27605**	0.38771	0.15049	**0.38206**	**0.29313**	0.37208	**0.37912**
	Hyperbolic	0.4382	0.482	0.31841	0.48837	0.45098	0.47109	0.49858
	Aly's	0.49049	0.52905	0.33879	0.55037	0.50022	0.51572	0.55229
VFPI	Passive Off	0.13571	0.15328	0.11074	0.15273	0.13752	0.14822	0.15898
	Passive On	0.54262	0.57614	0.35351	0.6032	0.54803	0.55371	0.6022
	Lyapunov	0.67022	**0.75302**	**0.48263**	**0.66454**	0.63589	0.6665	0.76391
	EMI	0.28644	0.3881	0.15054	0.38643	0.30001	0.35881	0.3823
	Hyperbolic	0.44462	0.48229	0.31814	0.492	0.45373	0.4675	0.49901
	Aly's	0.49558	0.53107	0.34192	0.55349	0.50345	0.51461	0.55323
VCFPS	Passive Off	0.13648	0.14982	0.11072	0.15382	0.13789	0.14029	0.15284
	Passive On	0.54319	0.57389	0.35335	0.60181	0.54872	0.55329	0.59864
	Lyapunov	**0.67242**	0.74941	0.48209	0.66453	**0.63618**	0.65896	**0.77046**
	EMI	0.29116	**0.38256**	**0.15018**	0.38931	0.30292	**0.34917**	0.3801
	Hyperbolic	0.44505	0.47696	0.31796	0.49136	0.45398	0.46479	0.49453
	Aly's	0.49635	0.52632	0.34196	0.55229	0.50399	0.51205	0.54881

It is observed that as the Lyapunov controlled MR dampers perform at higher forces consume more energy than EMI controlled MR dampers.

In summary, it can be concluded that the EMI based passive controller and local response controlled the Hyperbolic controller overall perform efficiently than the Lyapunov controller in base-isolated Irregular building with all types of isolation systems. VFPI and VCFPS isolation systems perform much better than FPS isolation system with MR damper control in base-isolated Irregular building.

6. CONCLUSIONS

Application of some passively controlled and local response governed control algorithms of MR dampers are compared with Lyapunov controller in base-isolated Irregular building. The Irregular building is subjected to strong near field earthquakes bi-directionally acting in the horizontal direction. The comparisons for different sliding-based isolation systems for controlled Irregular building have also been made. On the basis of observed trends of the results, following conclusions are made.

1. EMI based passive control and local response governed control algorithms are found comparable to Lyapunov controller in controlling the response of base-isolated Irregular building through MR dampers.
2. Smart passive control through EMI found reasonably efficient than Lyapunov controller though it restricts lesser base displacement but gives lower superstructure response.
3. Local response governed Hyperbolic controller also performed well as it controls base displacement comparable with Lyapunov controller but gives lower base shear and floor accelerations.
4. Aly's controller found not as useful as the other two controllers as it gives higher structural response with less reduction in base displacement.
5. VFPI and VCFPS isolation systems function efficiently with MR damper as compared to FPS isolation system. They produce not only give lower structural response but also give higher reduction in base displacement under controlled condition in base-isolated Irregular building.

Disclosures

Free Access to this article is sponsored by SARL ALPHA CRISTO INDUSTRIAL.

References

1. Hall, JF, Heaton, TH, Halling, MW, Wald, DJ. Near-source ground motion and its effects on flexible buildings. Earthquake Spectra 1995;11(4): 569-605.
2. Heaton, TH, Hall, JF, Halling, MW, Wald, DJ. Response of high-rise and base-isolated buildings to a hypothetical Mw 7.0 blind thrust earthquake. Science 1995; 67: 206-211.
3. Jangid, RS, Kelly, JM. Base isolation for near-fault motions. Earthquake Engineering and Structural Dynamics 2001; 30(5):691-707.
4. Agrawal, AK, Yang, JN, He WL. Applications of some semi-active control systems for an Irregular cable-stayed bridge. Journal of Structural Engineering (ASCE) 2003; 129(7):884–894.
5. He, WL, Agrawal, AK, Yang, JN. Novel semiactive friction controller for linear structures against earthquakes. Journal of Structural Engineering (ASCE) 2003; 129(7): 941–950.
6. Inaudi, JA. Modulated homogeneous friction: a semi-active damping strategy. Earthquake Engineering and Structural Dynamics 1997; 26: 361–76.
7. Spencer Jr., BF, Johnson, EA, Romello, JC. Smart isolation for seismic control. JSME International Journal, Series C 2000; 43(3), 704-711.
8. Spencer, BF, Nagarajaiah, S. State of the art of structural control. Journal of Structural Engineering (ASCE) 2003; 129(7):845–856.
9. Dupont, P, Kasturi, P, Stokes, A. Semiactive control of friction dampers. Journal of Sound and Vibration 1997; 202 (2): 203–218.
10. Fujita, T. Seismic isolation and response control for nuclear and non-nuclear structures. Special Issue for the Exhibition of 11th Int. Conf. on SMiRT Tokyo (Japan) 1991.
11. Symans, MD, Constantinou, MC. Semi-active control systems for seismic protection of structures: A state-of-the-art review. Engineering Structures *1999;* 21**:** 469-487.
12. Dyke, SJ, Spencer, BF Jr, Sain, MK and Carlson, JD. A New Semi-Active Control Device for Seismic Response Reduction. Proc. 11th ASCE Engg. Mech. Spec. Conf., 1996a, Ft. Lauderdale, Florida.
13. Dyke, SJ, Spencer, BF Jr, Sain, MK and Carlson, JD. Seismic Response Reduction Using Magnetorheological Dampers. *Proc. of the IFAC World Congress* 1996b, San Francisco, California.
14. Jung, HJ, Spencer, BF Jr, Lee, I W. Control of seismically excited cable-stayed bridge employing magnetorheological fluid dampers. Journal of Structural Engineering ASCE 2003; 129: 873-883.
15. Wang, Y, Dyke, S. Smart system design for a 3D base-isolated Irregular building. Structural Control and Health Monitoring 2008; 15(7): 939-957.
16. Yoshioka, H, Romello, JC, Spencer Jr, BF. Smart Base Isolation Strategies Employing Magnetorheological Dampers. Journal of Engineering Mechanics 2002; 128(5): 540-551.
17. Wen, Y.K., 1976. Method of Random Vibration of Hysteretic Systems. *Journal of Engineering Mechanics Division, ASCE,* 102, 249–263.
18. Stanway, R., Sproston, J.L., and Stevens, N.G., 1985. Non-linear Identification of an Electrorheological Vibration Damper. *IFAC Identification and System Parameter Estimation*, pp. 195– 200
19. Gamota, D.R., and Filisko, F.E., 1991. Dynamic Mechanical Studies of Electrorheological Materials: Moderate Frequencies. *Journal of Rheology*, Vol. 35, 399–425.
20. Brogan, W.L., 1991. *Modern Control Theory*, Prentice Hall, Englewood Cliffs, New Jersey.
21. Irschik, H., Schlacher, K., and Kugi, A., 1998. Control of earthquake excited nonlinear structures using Lyapunov's theory. Computers and Structures, 67, 83–90.
22. McClamroch, N.H. and Gavin, H.P., 1995. Closed Loop Structural Control Using Electrorheological Dampers. *Proc. of the Amer. Ctrl. Conf.*, Seattle, Washington, pp. 4173–77.
23. Dyke, S.J., Spencer Jr., B.F., Sain, M.K. and Carlson, J.D.1996c. Modelling and Control of Magnetorheological Dampers for Seismic Response Reduction. *Smart Materials and Structures,* 5, 565–575.
24. Dyke, S.J., 1996. Acceleration Feedback Control Strategies for Active and Semi-Active Systems: Modelling, Algorithm Development and Experimental Verification. Ph.D. Dissertation, University of Notre Dame, Notre Dame, IN.
25. Choi, K-M, Jung, H-J and Lee, I-W, 2004.Fuzzy control strategy for seismic response reduction of smart base isolated Irregular building. *17th ASCE Engineering Mechanics Conference,* University of Delaware, Newark DE.
26. Reigles D. G. and Symans, M D., 2006. Supervisory fuzzy control of a base-isolated Irregular building utilizing a neuro-fuzzy model of controllable fluid viscous dampers. *Structural Control and Health Monitoring*, 13,724–747.
27. Cho, S.W., Jung, H.J., and Lee, I.W., 2005. Smart passive system based on magnetorheological damper. *Smart Materials and Structures*, 14,707–714.
28. Pozo, F., Acho, L. and Rodellar, J., 2006. Hyperbolic control for vibration mitigation of a base-isolated Irregular structure. *Structural Control and Health Monitoring,* 16 (7-8), 766 – 783.
29. Aly, A. M., 2006. Vibration control of buildings under earthquake effects using MR Damper: a new control algorithm. *Alexandria University Journals*, http://fiu.academia.edu/documents/0073/2106/Paper_Aly_Mousaad_Alexandria_University.pdf
30. Narasimhan, S, Nagarajaiah, S, Johnson, EA, and Gavin, HP. Smart base isolated building Part I: Problem definition. Structural Control and Health Monitoring 2006*;*13: 573-588.
31. Pranesh, M. and Sinha, R., 2000. VFPI: An Isolation Device for Aseismic Design. *Earthquake Engineering and Structural Dynamics,* 29(5), 603-627.
32. Pranesh, M. and Sinha, R., 2004. Behaviour of torsionally coupled structures with variable frequency pendulum isolator. *Journal of Structural Engineering* (ASCE) 130, 1041-1054.

33. Tsai, C. S., Chiang T-C, and Chen B-J., 2003. Finite element formulations and theoretical study for variable curvature friction pendulum system. *Engineering Structures,* 25, 1719–1730.

34. Tsai, C.S., Chiang T-C, Chen B-J, and Chen K-C., 2005. Piecewise exact solution for analysis of base-isolated structures under earthquakes. *Structural Engineering and Mechanics,* 19(4), 381-399.

35. Spencer Jr., B.F., Dyke, S.J., Sain, M.K. and Carlson, J.D., 1997. Phenomenological model for magnetorheological dampers. *Journal of Engineering Mechanics* 123 (3), 230–238.

36. Chang, C.C. and Roschke, P., 1998. Neural network modelling of a magnetorheological damper. *Journal of Intelligent Material Systems and Structures,* 9 (9), 755–764.

37. Wereley, N.M. and Pang, Li, (1998). "Nondimensional analysis of semi-active electrorheological and magnetorheological dampers using approximate parallel plate models." *Smart Materials and Structures,* 7(5): 732-743.

38. Schurter, K.C., and Roschke, P.N., 2000. Fuzzy modelling of a magnetorheological damper using ANFIS. In Proceedings of IEEE International Conference on Fuzzy Systems, 122–127

39. Choi, S.B., Lee, S.K., and Park, Y.P., 2001. A hysteresis model for the field-dependent damping force of a magnetorheological damper. *Journal of Sound and Vibration,* 245 (2), 375–383.

40. Jung, H-J, Spencer Jr, BF, Lee, I-W. Control of seismically excited cable stayed bridge employing Magnetorheological fluid dampers. Journal of Structural Engineering ASCE 2003; 129(7): 873-883.

41. Dyke, SJ, Spencer, Jr, BF. A Comparison of semi-active control strategies for the MR damper. Proceedings of the IASTED International Conference, Intelligent Information Systems, December 8–10, 1997, Bahamas.

42. Reitz, J. R., Milford, F. J., and Christy, R. W., 1993. *Foundations of Electromagnetic Theory* (Reading, MA: Addison-Wesley).

43. Marshall, S. V., and Skitek, G. G., 1990. *Electromagnetic Concepts and Applications* (Englewood's Cliffs, NJ: Prentice-Hall)

44. Miner, G. F., 1996. *Lines and Electromagnetic Fields for Engineers* (Oxford: Oxford University Press)

45. Yang, G., Spencer, B.F. Jr., Carlson, J.D. and Sain, M.K., (2002). Large scale MR fluid dampers: modelling and dynamic performance considerations. *Engineering Structures*, 24, 309-323.